

PAPER • OPEN ACCESS

## Interaction of shock waves with elastic-plastic medium

To cite this article: Sherzod Khudainazarov *et al* 2020 *IOP Conf. Ser.: Mater. Sci. Eng.* **869** 052074

View the [article online](#) for updates and enhancements.

# Interaction of shock waves with elastic-plastic medium

**Sherzod Khudainazarov<sup>1</sup>, Burxon Donayev<sup>2</sup>, Erkin Abdimuminov<sup>2</sup> and Yulduz Suyunova<sup>2</sup>**

<sup>1</sup>Tashkent Institute of Irrigation and Agricultural Mechanization Engineers, 39, Kori Niyoziy str., Tashkent, Uzbekistan, 100000

<sup>2</sup>Karshi Engineering-Economics Institute, 225, Mustakillik str., Karshi, Uzbekistan.

E-mail: schertzodshox77@mail.ru

**Abstract** The problem of spherical shock wave propagation in an elastic-plastic medium is solved analytically and numerically by the method of characteristics on the basis of the strain theory, including the generalized equations of state of the medium. The spherical shock wave propagation in an elastic-plastic medium with a more complex equation of state for the medium forming is studied. The results show that an account for nonlinear-elastic shock diagrams leads to an increase in circular stress wave compared to an elastic medium. It was found that the stress concentration is higher on the spherical cavity than on the cylindrical one.

## 1. Introduction

Recently, fast-running wave processes and as a result, the cases of intense short-term loads are often found in many fields of science and technology, in particular, in aircraft manufacturing, shipbuilding, rocket engineering, mechanical engineering, seismology and earthquake-resistant construction. In the practice of civil and industrial construction this is connected with the erection of various hydro-technical and underground structures of spherical and cylindrical shapes in seismically dangerous zones, using an explosion in the mining, with predicting the strength of structures, machines, units and massifs subject to dynamic (including seismic and explosive) high-intensity impacts, and with the development of theoretical and experimental methods for calculating their stress-strain states considering wave diffraction.

In this case, a special place is occupied by the study of the wave interaction with a structure or a formation in the case when the structure (unit) and the environment undergo irreversible strains, i.e. when the stress-strain state of the system in question is, on the whole, beyond elasticity. In this case, to determine the dynamic loads from the above mentioned effects on various structures, it is necessary, first of all, to study the nonlinear waves propagation in the medium and its kinematic parameters, and then to study the processes of wave diffraction from the surface of structures considering the properties of the structure material. However, the problem under consideration is three-dimensional and non-stationary one, therefore, the methods for calculating underground structures on dynamic impacts due to the complexity of physical and mathematical properties of soil, the nature of seismic and explosive effects, the shape and geometry of structures have not yet been developed. However, from the simplified methods of studying this problem, the study of non-stationary processes can be



carried out in one- and two-dimensional statements. Some success has been achieved in this direction using a barrier of various shapes within the framework of the nonlinear theory of elasticity. Despite this, a limited number of publications are devoted to similar studies on elastic-plastic strains.

In [10–13], the characteristics of a shock wave propagation caused by a gas detonation wave emerging from the open end of a cylindrical detonation tube were investigated experimentally. The results were obtained using dimensionless pressure and distance, which did not depend of the mixture diversity and pipe diameter. Based on the results of the studies, it was determined that an account of viscosity leads to wave attenuation. Subsequently, the shock wave attenuates more rapidly than the ideal sound attenuation, turning from a quasi-spherical wave to a spherical one.

In [14–15], the propagation of a spherical wave in linear-elastic and viscoelastic media was studied. There, for modeling viscoelastic damping, a new model and a new approach to the analytical solution of the problem were developed. Wave propagation is achieved by cascading individual mechanisms of geometrical attenuation and viscoelastic attenuation. Comparison of the analytical model with the results of dynamic finite element modeling shows that the cascading method of individual transfer functions is an appropriate approach for the wave propagation in viscoelastic medium.

Propagation of isolated spherical blast waves in the form of point explosions and gas explosions under high pressure were considered in [16-17]. The test data on the explosion overpressure as a result of interaction of spherical blast waves initiated from explosives in the form of cumulative charges of various strengths were presented. The results were discussed with the laws of scaling relating to the reduction of explosion overpressure and indicated the possibility of detecting a source explosion by pressure measurements in the far zone.

In [18], modeling of soil fragmentation during underground explosions was studied and a modified smoothed particle hydrodynamics method (SPH) was introduced. To solve interphase problems with high density coefficients, a modified continuity equation was used. To describe the mechanical behavior of the, elastic and hypo-plastic constitutive models were used. The obtained simulation results were compared with experimental data, which showed that the smoothed particle hydrodynamics method SPH in combination with these two basic models can solve the problems of detonation of landmines associated with large strain.

In [19-22], the methods for propagation damping of strong spherical waves were investigated and dynamic calculations of structures supported on a layer of a sand base subjected to explosive effects of soil were carried out. Numerical results show that the use of a sand base is effective in reducing the structural response and damage from ground movements caused by an explosion, both at high and relatively low frequencies, even though the effects of insulation tend to decrease with a decrease in fundamental frequency of ground motion.

In this regard, in this paper, the one-dimensional and two-dimensional non-stationary problems of dynamic theory of plasticity are studied as applied to the calculation of medium parameters in the cases of wave propagation and deformation from a different surface, based on a deformation theory with more complex equations of state.

## 2. Methods

The problem of wave propagation in soil under the action of intense monotonically decreasing load  $\sigma_0(t)$  applied to the boundary of a cavity radius is considered. Soil at high stresses is modeled as an elastic-plastic medium considering the linear irreversible unloading of the medium. To describe the motion of a medium, a deformation theory [1] is used with determining functions  $\sigma = \sigma(\varepsilon)$ ,  $\sigma_i = \sigma_i(\varepsilon_i)$ , where  $\varepsilon$ ,  $\varepsilon_i$ ,  $\sigma$ ,  $\sigma_i$  are the first and second invariants of the strain and stress tensors.

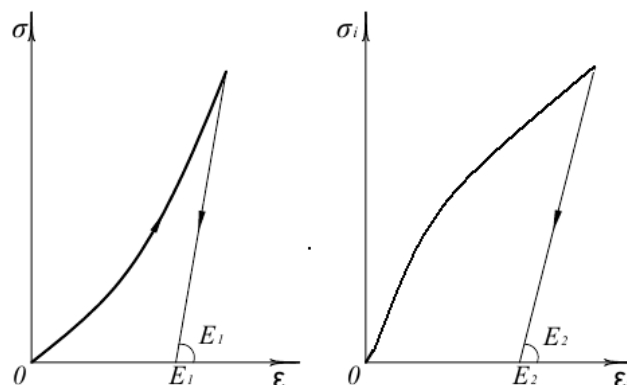


**Figure 1.** Change in the first and second invariants of the stress  $\sigma$ ,  $\sigma_i$  and strain  $\varepsilon$ ,  $\varepsilon_i$  tensors

These functions in the process of loading the medium are presented in the form of polynomials in which constant coefficients  $\alpha_i$ ,  $\beta_i$  ( $i = 1,2$ ) are determined experimentally considering the triaxial stress state of soil.

$$\sigma(\varepsilon) = (\alpha_1 + \alpha_2|\varepsilon|)\varepsilon\sigma_i(\varepsilon_i) = (\beta_1 - \beta_2\varepsilon_i)\varepsilon_i \quad (1)$$

The solution to the problem is constructed analytically by the inverse method for a given surface shape of the shock wave in the form of a polynomial of the second degree with respect to time  $t$  and numerically by the method of characteristics for a given randomly decreasing load  $\sigma_0(t)$ . Based on the obtained analytical formulas, the parameters of the medium are calculated on the computer, including the load profile and the comparison of stresses, mass velocity of plastic and elastoplastic medium.

Let a monotonically decreasing load  $\sigma_0(t)$  be applied to the boundary of a spherical cavity  $r = r_0$ . In the case under consideration, the problem within the framework of the deformation theory of soil plasticity [3], the equation of motion of the medium

$$\rho_0 \frac{\partial^2 U}{\partial t^2} = \frac{\partial \sigma_{rr}}{\partial r} + 2 \frac{(\partial \sigma_{rr} - \sigma_{\varphi\varphi})}{r} \quad (2)$$

considering dependence between stress and strain components

$$\sigma_{rr} = \varepsilon\lambda + 2G\varepsilon_{rr}, \sigma_{\varphi\varphi} = \sigma_{\theta\theta} = \varepsilon\lambda + 2G\varepsilon_{rr}, \varepsilon = \frac{\partial u}{\partial r} + 2\frac{u}{r} \quad \lambda = \frac{\sigma}{\varepsilon} - \left(\frac{2}{9}\right)\frac{\sigma_i}{\varepsilon_i}, G = \left(\frac{1}{3}\right)\frac{\sigma_i}{\varepsilon_i} \quad (3)$$

takes the form

$$\rho_0 \frac{\partial^2 U}{\partial t^2} \left\{ \left( \alpha_1 + \frac{4}{9}\beta_1 \right) - 2 \left( \alpha_2 - \frac{8}{27}\beta_2 \right) \frac{\partial U}{\partial r} - 4 \left( \alpha_1 + \frac{2}{9}\beta_2 \right) \frac{U}{r} \right\} \frac{\partial^2 U}{\partial r^2} + \frac{Q_0 \left( \frac{\partial U}{\partial r} \cdot U \cdot r \right)}{r} \quad (4)$$

where

$$Q_0 \left( \frac{\partial U}{\partial r} \cdot U \cdot r \right) 2 \left\{ \frac{2}{3}\beta_1 \frac{\partial U}{\partial r} + \left[ \left( \alpha_1 - \frac{2}{9}\beta_1 \right) - 2 \left( \alpha_2 + \frac{5}{9}\beta_2 \right) \right] \frac{\partial U}{\partial r} - \left[ \left( \alpha_2 + \frac{2}{27}\beta_2 \right) \frac{U}{r} \right] \left( \frac{\partial U}{\partial r} - \frac{U}{r} \right) \right\}$$

We introduce the notation

$$\alpha^2 = \left[ \left( \alpha_1 + \frac{4}{9}\beta_1 \right) - 2 \left( \alpha_2 - \frac{8}{27}\beta_2 \right) \frac{\partial U}{\partial r} - 4 \left( \alpha_2 - \frac{2}{9}\beta_2 \right) \frac{U}{r} \right] / \rho_0 \quad (5)$$

From (5) at  $U=0$   $\frac{\partial U}{\partial r} = 0$  we have  $\alpha_{01} = \sqrt{(\alpha_1 + \frac{4}{9}\beta_1) / \rho_0}$

where  $\alpha_{01}$  is the velocity of the elastic wave;  $\alpha$  - variable wave velocity

Research (4) shows that at  $(\alpha_2 - \frac{8}{27}\beta_2) > 0$ , according to the condition for the existence of a shock wave (4) (at the front of the shock wave the displacement is  $U = 0$ ), a shock wave propagates in soil  $r = R(t)$  (Fig. 2.)

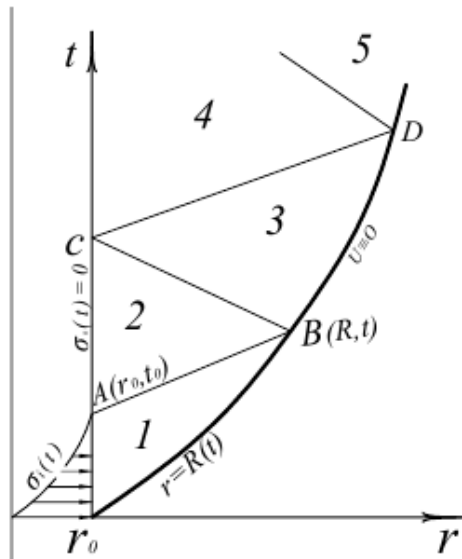


**Figure 2.** Graph of shock wave propagation in soil  $r=R(t)$ .

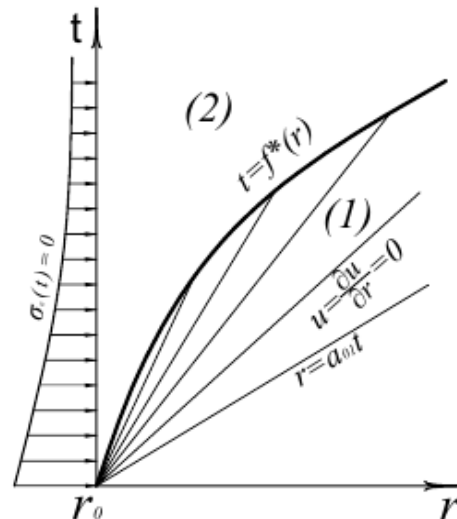


**Figure 3.** Changes in the unloading wave  $t = f^*(r)$  at the boundary of the medium loading and unloading

otherwise, at  $(\alpha_2 - \frac{8}{27}\beta_2) < 0$ , the centered Riemann loading waves, which are cut off from above by the unloading wave  $t = f^*(r)$ , which is the boundary of the region of loading and unloading of the medium (Fig. 3.)

Since the shock wave is a load-unloading wave and the medium is unloaded behind its front, then from (2), considering the unloading theorem of A.A. Ilyushin, expressed by the formula

$$\begin{aligned} \sigma_{rr} &= \sigma_{rr}^*(r) + \lambda_0(\varepsilon - \varepsilon^*(r)) + 2G_0(\varepsilon_{rr} - \varepsilon_{rr}^*(r)) \\ \sigma_{\varphi\varphi} &= \sigma_{\varphi\varphi}^*(r) + \lambda_0(\varepsilon - \varepsilon^*(r)) + 2G_0(\varepsilon_{\varphi\varphi} - \varepsilon_{\varphi\varphi}^*(r)) \end{aligned} \tag{6}$$

we get the equation

$$\frac{\partial^2 U}{\partial t^2} = \alpha_0^2 \left[ \frac{\partial^2 U}{\partial r^2} + \frac{2}{r} \left( \frac{\partial U}{\partial r} - \frac{U}{r} \right) + \frac{Q(r)}{\rho_0 \alpha_0^2} \right] \tag{7}$$

$$\begin{aligned} Q(r) &= \frac{\partial}{\partial U} [\sigma_{rr}(r) - \rho_0 \alpha_0^2 \varepsilon^*(r)] + \frac{2}{r} [\sigma_{rr}^*(r) - \sigma_{\varphi\varphi}(r) - 2G_0 \varepsilon^*(r)] \\ \rho_0 \alpha_0^2 &= \lambda_0 + 2G_0 \end{aligned} \tag{8}$$

$$\lambda_0 = E_1 - \frac{2}{9}E_2, \quad G_0 = \frac{1}{3}E_2, \quad \alpha_0 = \sqrt{(E_1 + \frac{4}{9}\beta_1)/\rho_0}$$

Where,  $E_1, E_2$ - tangents of the angles of inclination of the branches of rectilinear unloading of diagrams  $\sigma(\varepsilon)$  and  $\sigma_i(\varepsilon_i)$ , respectively with the axes  $\varepsilon$  and  $\varepsilon_i$ ,  $U$  – is the displacement. Front parameters of the medium are indicated by an asterisk.

Consider the case  $(\alpha_2 - \frac{8}{27}\beta_2) > 0$ . In this case, the conditions at the wave front of the cavity boundary have the form

$$\sigma_{rr}^* = -\rho_0 R^I(t) U_t^* \quad U_t^* = -R^I(t) \varepsilon_{rr}^* \tag{9}$$

$$\begin{aligned} U(r, t) &= 0 \text{ at } r = R(t) \quad \sigma_{rr} = \sigma_0(t) \text{ at } r = r_0 \quad t \geq 0 \\ \text{where } U_t &= \frac{\partial U}{\partial t} = U^I \quad R^I(t) = \frac{\partial R}{\partial t} \end{aligned} \tag{10}$$

As was said above, the solution to the problem is constructed in the reverse way, therefore, it is assumed that  $R(t)$  is given and in solution course, the load profile is determined using  $\sigma_0(t)$ . Then  $R^I(t)$  considering (3) at  $r = R(t)$  takes the form:

$$\varepsilon_0^*(t) = \varepsilon_{rr}(t) = -\frac{\rho_0 R^2(t) - (\alpha_1 + \frac{4}{9}\beta_1)}{(\alpha_2 - \frac{8}{27}\beta_2)}, \tag{11}$$

$$U_t^* = R(t)\varepsilon^*(t)$$

Using the d'Alembert formulas, the solution of equation (7) can be represented as:

$$U(r, t) = \frac{\psi^*(r-\alpha_0 t) + \phi(r+\alpha_0 t)}{r} - \frac{\psi(r-\alpha_0 t) + \phi(r+\alpha_0 t)}{r^2} - \frac{r}{3(\lambda_0 + 2G_0)} \int_{r_0}^r Q(r) dr + \frac{1}{3(\lambda_0 + 2G_0)r^2} \int_{r_0}^r Q(r)r^3 dr \tag{12}$$

Where  $\psi$  and  $\phi$  are the unknown functions.

Substituting (12) into (11) to determine the sought for functions  $\psi$  and  $\phi$  we obtain a system of ordinary differential equations of the form:

$$\frac{\psi^{II}[R(t)-\alpha_0 t] + \phi[R(t)+\alpha_0 t]}{R(t)} - 2 \frac{\psi^I[R(t)-\alpha_0 t] + \phi^I[R(t)+\alpha_0 t]}{R^2(t)} + 2 \frac{\psi[R(t)-\alpha_0 t] + \phi[R(t)+\alpha_0 t]}{R^3(t)} - \frac{1}{3(\lambda_0 + 2G_0)} \int_{r_0}^{R(t)} Q(r) dr - \frac{2}{3(\lambda_0 + 2G_0)R^3(t)} \int_{r_0}^{R(t)} r^3 Q(r) dr = -\frac{\rho_0 R^2(t) - (\alpha_1 + \frac{4}{9}\beta_1)}{(\alpha_2 - \frac{8}{27}\beta_2)} \tag{13}$$

$$\frac{-\psi^{II}[R(t)-\alpha_0 t] + \phi^{II}[R(t)+\alpha_0 t]}{R(t)} - \frac{\psi^I[R(t)-\alpha_0 t] + \phi^I[R(t)+\alpha_0 t]}{R^2(t)} = \frac{R(t)}{\alpha_0} \left[ \frac{\rho_0 R^2(t) - (\alpha_1 + \frac{4}{9}\beta_1)}{(\alpha_2 - \frac{8}{27}\beta_2)} \right] \tag{14}$$

Further, considering that at the shock front  $r = R(t)$ , displacement  $U(r, t) = 0$  we get:

$$\frac{\psi^{II}[R(t)-\alpha_0 t] + \phi^{II}[R(t)+\alpha_0 t]}{R(t)} = -\frac{[\rho_0 R^2(t) - (\alpha_1 + \frac{4}{9}\beta_1)]}{(\alpha_2 - \frac{8}{27}\beta_2)} + \frac{1}{(\lambda_0 + 2G_0)} \int_{r_0}^{R(t)} Q(r) dr \tag{15}$$

Substituting (14) and (15) and differentiating by  $t$  we have

$$\psi^{III}[R(t) - \alpha_0 t] = \frac{1}{2\alpha_0(\alpha_2 - \frac{8}{27}\beta_2)(\alpha_0 - R(t))} * \{ [(2R^I(t) - \alpha_0)(R(t) + \alpha_0) + R(t)R^{II}(t)] [\rho_0 R^2(t) - (\alpha_1 + \frac{4}{9}\beta_1)] + 2\rho_0 R^I(t)(R^I(t) + \alpha_0)R^{II}(t) \} - \frac{R(t)(R^I(t)Q(R(t)))}{(\alpha_0 - R^I(t))(\lambda_0 + 2G_0)} + \frac{1}{2(\lambda_0 + 2G_0)} \int_{r_0}^{R(t)} Q(r) dr \tag{16}$$

If we introduce the notation  $R(t) - \alpha_0 t = Z$  then (16) takes the form

$$\psi^{III}(Z) = \phi_2(Z)$$

$$\phi_2(Z) = \left\{ [(2R^I(F_1(Z)) - \alpha_0)(R^I(F_1(Z)) + \alpha_0) + R(F_1(Z)) * R^{II}(F_1(Z)))] [\rho_0 R^2(F_1(Z))] - (\alpha_1 + \frac{4}{9}\beta_1) + 2\rho_0 R(F_1(Z))R^I(F_1(Z) + \alpha_0)R^{II}(F_1(Z)) \right\} - \frac{R(F_1^{(Z)})(R(F_1^{(Z)}))Q(R(F_1^{(Z)}))}{(\alpha_0 - R^I(F_1))2(\lambda_0 + 2\sigma_0)} + \frac{1}{2(\lambda_0 + 2G_0)} \int_{r_0}^{R(F_1^{(Z)})} Q(r) dr \tag{17}$$

After that, the solution of the problem regarding the displacement  $U(r, t)$  considering (11) is written in the form:

$$\begin{aligned}
 & U(r, t) \\
 = & \frac{1}{r} \left\{ \int_{r_0}^{r-\alpha_0 t} d\xi_2 \int_{r_0}^{\xi_2} \phi_2(\xi_1) d\xi_1 - \int_{r_0}^{r-\alpha_0 t} d\xi_2 \int_{r_0}^{R(F_2(\xi_2))-\alpha_0(F_2(\xi_2))} \phi_2(\xi_1) d\xi_1 \right. \\
 & + \left. \int_{r_0}^{r+\alpha_0 t} \frac{R(F_2(\xi_2))}{(\lambda_0 + 2\sigma_0)} d\xi_2 \int_{r_0}^{R(F_2(\xi_2))} Q(\xi) \partial \xi_1 - \int_{r_0}^{r+\alpha_0 t} \frac{R(F_2(\xi_2)) \rho_0 R^2(F_2(\xi_2)) - (\alpha_2 + \frac{4}{9} \beta_1)}{(\alpha_2 - \frac{8}{27} \beta_2)} d\xi_2 \right\} - \\
 & - \frac{1}{r^2} \left\{ \int_{r_0}^{r-\alpha_0 t} d\xi_3 \int_{r_0}^{\xi_2} d\xi_2 \phi_2 \int_{r_0}^{\xi_2} (\xi_1) d\xi_1 - \frac{\alpha_0 r_0^2 (1 + \frac{R(0)}{\alpha_0})}{\alpha_2 - \frac{8}{27} \beta_2} \right\} * \left[ \rho_0 R^2(0) - \left( \alpha_1 + \frac{4}{9} \beta_1 \right) \right] t - \\
 & \int_{r_0}^{r+\alpha_0 t} d\xi_3 \phi_2 \int_{r_0}^{\xi_3} \frac{R(F_2(\xi_2)) \rho_0 R^2(F_2(\xi_2)) - (\alpha_1 + \frac{4}{9} \beta_1)}{(\alpha_2 - \frac{8}{27} \beta_2)} d\xi_2 + \int_{r_0}^{r+\alpha_0 t} d\xi_3 \int_{r_0}^{\xi_3} \frac{R(F_2(\xi_2))}{(\lambda_0 + 2G_0)} d\xi_3 \int_{r_0}^{R(F_2(\xi_2))} Q(\xi_1) d\xi_1 - \\
 & \frac{r}{3(\lambda_0 + 2G_0)r^2} \int_{r_0}^r Q(\xi) \xi^3 \partial \xi_3 * \int_{r_0}^r Q(r) dr + \frac{1}{3(\lambda_0 + 2\sigma_0)} \int_{r_0}^r Q(\xi) \xi^2 d\xi \tag{18}
 \end{aligned}$$

where  $F_i(Z_i) - (i=1,2)$  is the root of the equation  $R(t) \pm \alpha_0 t = Z_i$  relative to time  $t$ ;

$\phi_2(z)$  is a well-known function of its argument, expressed in terms of the parameters of the medium at the shock wave front.

Differentiating the equation (18) by time  $t$  and  $r$  we determine the mass velocity  $U_t(r,t)$  and the strain  $\varepsilon(r, t)$ , and then, based on formulas (6), the stress components  $\sigma_{rr}, \sigma_{\varphi\varphi}$  are calculated. Further, substituting (6) considering (18) into (10) we find the load profile  $\sigma_0(t)$ . Note that the expressions are valid as long as  $\sigma_0(t) \geq 0$ . In the future, in the case of  $\sigma_0(t) \equiv 0$ , it is necessary to solve the corresponding boundary value problems.

### 3. Results and discussion

To do this, we carry out the characteristics of AB, BC, CD, etc. Then, the region under consideration is divided into  $n = 1, 2, 3$  (Fig. 2) regions, each of which for  $n \geq 2$  is limited by the characteristics of the positive, negative directions and the boundary of the cavity or part of the wave front  $r = R(t)$ . Solving problems for regions 2 and 3 (Fig. 2.), as well as for subsequent areas, can be obtained according to the methodology of work [5].

In addition, further studies show that the above inverse method becomes relatively effective in studying wave processes near the boundary of a spherical cavity, i.e. in the vicinity of the point  $r = r_0, t=0$  in the plane  $(r, t)$  (Fig. 4).

Indeed, in a sufficiently small time interval, varying the law of velocity change of the spherical wave  $\dot{R}(t)$  in time by the selection method, with a certain accuracy, we can achieve the specified law of time decay of the load  $\sigma_0(t)$ . In this case, the wave pattern of the problem takes the form shown in Fig. 4.

Considering that the solution to the problem for the form of region 1 (Fig. 4) was obtained above in the reverse way and the displacement of the medium in this region was calculated using formula (18), we proceed to the description of the solution to the problem for regions 2 and 3.

Let us present a solution to the problem for region 2. In this case, from (7), based on the d'Alembert formula, it is easy to obtain

$$\begin{aligned}
 & U_2(r, t) = \\
 & \frac{\psi_2^J(r-\alpha_0 t) + \phi_2^J(r+\alpha_0 t)}{r} - \frac{\psi_2(r-\alpha_0 t) + \phi_2(r+\alpha_0 t)}{r^2} - \frac{r}{3(\lambda_0 + 2G_0)} \int_{r_0}^r Q(r) dr + \frac{1}{3(\lambda_0 + 2\sigma_0)r^2} \int_{r_0}^r r^3 Q(r) dr \tag{19}
 \end{aligned}$$

To find  $\psi_2(z)$  and  $\phi_2(z)$ , we have the conditions

$$\frac{\partial U_2}{\partial t} = U_1(t) \quad \frac{\partial U_2}{\partial r} = \varepsilon_{rr}(t) \quad r - r_0 = \alpha_0(t - t_0) \tag{20}$$

$U_2 = U_1(t)$  at  $\sigma_{rr}(r, t) = -\sigma_0(t)$  at  $r = r_0 \quad t_\alpha \leq t \leq t_c$  (21)  
 where  $U_1(t), U_1(t), \varepsilon_{rr}(t)$  - is the displacement, velocity and radial strain in soil on the AB characteristic (Fig. 4), determined from solving problems in region 1.

Substituting (19) into (20) and (21), considering (6), we obtain

$$\psi_2(z) = \frac{1}{\omega} e^{\sigma_1 z} \left[ \sin \omega z \int_{r_0 - \alpha_0 t_\alpha}^z M(Z) e^{\sigma_{1z}} \cos \omega z dz - \cos \omega z * \int_{r_0 - \alpha_0 t_\alpha}^z M(Z) e^{\sigma_{1z}} \sin \omega z dz \right] \tag{22}$$

$$\phi_2(z) = \frac{U_1(t_\alpha)}{12r_0} [Z + (r_0 - \alpha_0 t_\alpha)] + \int_{r_0 - \alpha_0 t_\alpha}^z [Z + (r_0 - \alpha_0 t_\alpha)] \int_{r_0 + \alpha_0 t_\alpha}^z \frac{N(\xi)}{[\xi + (r_0 - \alpha_0 t_\alpha)]} 2d\xi dz; \tag{23}$$

where

$$N(z) = \frac{U_1 \frac{z - (r_0 - \alpha_0 t_\alpha)}{2\alpha_0}}{2\alpha_0} [Z + (r_0 - \alpha_0 t_\alpha)] + \frac{1}{2} \left[ \varepsilon_1(t_\alpha) r_0 - \frac{U_1(t_\alpha)}{\alpha_0} r_0 - U_1(t_\alpha) \right] \tag{24}$$

$$M(z) = -\sigma_0 \left( \frac{r_0 - z}{\alpha_0} \right) - \sigma_{rr}^*(r_0) + (\lambda_0 + 2G_0) \varepsilon_{rr}^*(r_0) - \frac{(\lambda_0 + 2G_0)}{r_0} \phi_2^I(2r_0 - z) + \frac{4G_0}{r_0^3} \phi_2(2r_0 - z) - \frac{4G_0}{r_0^3} \phi_2^I(2r_0 - z)$$

$$l_0 = \frac{\lambda_0 + 2G_0}{r}, \quad l_1 = \frac{4\sigma_0}{r_0^2}, \quad l_2 = \frac{4\sigma_0}{r_0^3}, \quad \sigma_1 = \frac{l_1}{2l_0} \quad \omega = \sqrt{\frac{4l_0 l_2 - l_1^2}{2l_0}}$$

Therefore, substituting (22) and (23) into (20) considering (24), the displacement  $U_2(r, t)$  is determined after differentiating (20) the velocity  $U_2^I(r, t)$  and the strain components  $\varepsilon_{rr_2}(r, t), \varepsilon_{\varphi\varphi_2}(r, t), \varepsilon_2(r, t)$  including volume strain of soil in region 2. Further, formulas (6) make it possible to determine the components of soil stresses in region 2:

$$\sigma_{rr_2}(r, t) \sigma_{\varphi\varphi_2}(r, t) = \sigma_{\theta\theta_2}(r, t)$$

Proceed to solving the problem in region 3. We represent the solution of the equation (7) in region 3 in the form

$$U_3(r, t) = \frac{\psi_3^1(r - \alpha_0 t) + \phi_3^1(r + \alpha_0 t)}{r} - \frac{\psi_3(r - \alpha_0 t) + \phi_3(r + \alpha_0 t)}{r^2} - \frac{r}{3(\lambda_0 + 2G_0)} \int_{r_b}^r Q(r) dr + \frac{1}{3(\lambda_0 + 2G_0)r^2} \int_{r_b}^r r^3 Q(r) dr \tag{25}$$

It should be noted that in [6], when studying the propagation of a one-dimensional plastic wave in soils, it was found that the front of the shock wave as a function of time is almost straight, although the parameters of the medium vary significantly. The curvature of the front in the considered time interval is approximately 15-20% of the initial state. Consider this circumstance and the finiteness of the length of section BD, in a first approximation, the ratios on the surface of the shock wave  $r = R(t)$  are satisfied relative to the initial shape of the front corresponding to the point  $B(r_b, t_b)$ .

Then we have:

$$\frac{\partial U}{\partial t} = U_2^I(t), \quad \frac{\partial U_3}{\partial r} = \varepsilon_{rr}(t), \quad U_3(r, t) = U_2(t) \quad \text{at} \quad r + \alpha_0 t = r_b + \alpha_0 t_b$$



$$r - r_b = R^I(t_b)(t - t_b) \text{ at } \begin{cases} \varepsilon_3^*(t) = -\frac{[\rho_0 R^2(t) - (\alpha_1 + \frac{4}{9}\beta_1)]}{(\alpha_2 - \frac{8}{27}\beta_2)} \\ \frac{\partial U_3^*}{\partial t} = R_0^I(t) \frac{[\rho_0 R^2(t) - (\alpha_1 + \frac{4}{9}\beta_1)]}{(\alpha_2 - \frac{8}{27}\beta_2)} \end{cases} \quad (26)$$

where  $U_2(t), U_2^I(t), \varepsilon_{rr_2}(t)$  is the displacement, velocity, and radial strain of the medium on the aircraft, determined from the solution of the problem in region 2.

Expressions (26) and (27) with (20) allow to determine the required functions  $\psi_3(r - \alpha_0 t), \phi_3(r + \alpha_0 t)$  and  $R_0^I(t)$  in region 3. Proceed to the solution of problems in the region 3. Solutions (7) of the region represented in the form:

$$U_3(r, t) = \frac{\psi_3^I(r_0 - \alpha_0 t) + \phi_2^II(r_0 + \alpha_0 t)}{r} - \frac{\psi_3(r_0 - \alpha_0 t) + \phi_2(r_0 + \alpha_0 t)}{r^2} - \frac{r}{3(\lambda_0 + 2G_0)} \int_{r_b}^r Q(r) dr + \frac{1}{3(\lambda_0 + 2G_0)r^2} \int_{r_b}^r r^3 Q(r) dr \quad (27)$$

where  $r_b$ -is the coordinate of the point B. To find the functions  $\psi_3(z)$  and  $\phi_3(z)$ , the problem has a boundary condition on

$$\psi_3(z) = \frac{C_5}{3} [z + (r_b + \alpha_0 t_b)]^3 + \int_{r_b - \alpha_0 t_b}^z [z + (r_b + \alpha_0 t_b)]^2 * \int_{r_b}^z -\alpha_0 t_b \frac{N_1(\xi)}{[\xi_1 + (r_b + \alpha_0 t_b)]^2} d\xi dz + C_6 \quad (28)$$

$$\begin{aligned} \phi_3(z) = \\ \frac{C_7}{(x+1)} \left[ Z + \frac{\alpha_0}{R(t_b)} (r_b - R(t_b)t_b) \right]^{x-1} + \int_{r_b + \alpha_0 t_b}^z \left[ Z + \frac{\alpha_0}{R(t_b)} (r_b - R(t_b)t_b) \right]^x * \\ \int_{r_b + \alpha_0 t_b}^z \frac{M_1(\xi)}{\left[ Z + \frac{\alpha_0}{R(t_b)} (r_b - R(t_b)t_b) \right]} d\xi dz + C_8 \end{aligned} \quad (29)$$

where  $x = (1 + \frac{\alpha_0}{R(t_b)}) > 2$ ,  $C_5, C_6, C_7, C_8$  – are the arbitrary constant coefficients, determined from the conditions of problem (26) and (27) for  $r = r_b, t = t_b$ , i.e. at point B (Fig. 4)

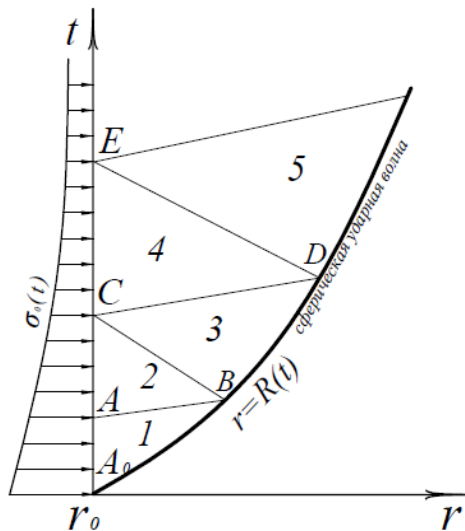


**Figure 4.** Change in a spherical shock wave in the vicinity of the point  $r = r_0$

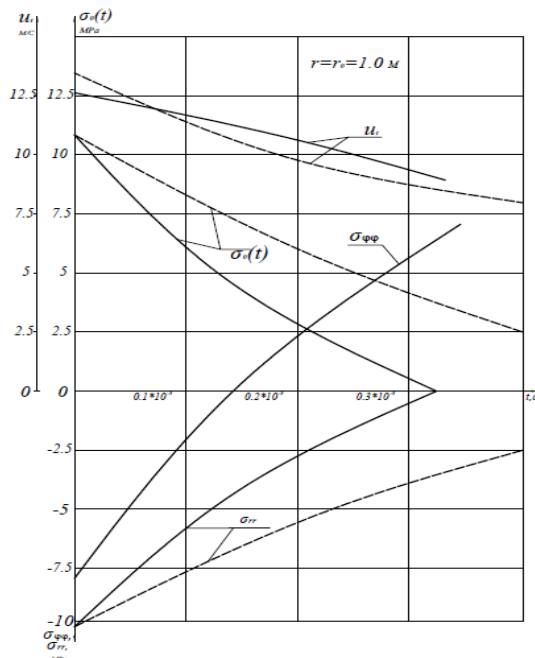


**Figure 5.** Change in stresses  $\sigma_{rr}, \sigma_{\phi\phi}$  of mass velocity  $U_t$  and load  $\sigma_0(t)$  at the boundary of the spherical cavity  $r = r_0 = 1$ .

The calculations were carried out for the case when the surface shape of the shock wave, for the beginning of the wave process, is set in the form of a polynomial of the second degree

$$R(t) = r_0 + R_1 t - \left(\frac{R_2}{2}\right)t^2 \text{ where } R(t) > 0, \text{ and initial parameters in the form (29)}$$

$$\rho_0 = \frac{2 \text{ kN sec}^2}{\text{m}^4} \quad \sigma_0(0) = 10.5 \text{ MPa} \quad r_0 = 1 \text{ m} \quad R_1 = 391 \frac{\text{m}}{\text{sec}} \quad \text{or} \quad 420 \frac{\text{m}}{\text{sec}} \quad R_2 = 2 * 10^2 * R_1 \left(\frac{\text{m}}{\text{sec}^2}\right), \quad \alpha_1 = 1.2127 * 10^4 \text{ MPa}, \quad \alpha_2 = 5.873 * 10^3 \text{ MPa}, \quad \beta_1 = 3.538 * 10^2 \text{ MPa}, \quad \beta_2 = 1.164 * 10^4 \text{ MPa}, \quad E_1 = 1.4 * 10^3 \text{ MPa}, \quad E_2 = 0.2 * 10^3 \text{ MPa}$$

The results of computer calculations are presented in Figs. 5-8 in the form of graphs of stresses, mass velocity and load depending on time and spatial coordinate  $r$ , as well as on the shock front  $r = R(t)$ . Here, the dashed and solid lines correspond respectively to an ideal nonlinearly compressible and elastoplastic media, and the results of the method characterizing the elastoplastic problem are indicated by a dashed line with points. Calculations at  $t = 0$  considering relations (9) in the case of fulfilling the boundary condition.

$$\sigma_{rr}(r_0, 0) = -P(r_0, 0) = \sigma_0(0) = 10.5 \text{ MPa}$$

show that the shock wave velocity  $R^I(0) = R_1$  for non-linearly compressible [7] and elastoplastic media is different and equal to  $R_1 = 391 \frac{\text{m}}{\text{sec}}$  or  $420 \frac{\text{m}}{\text{sec}}$ , respectively.

Consequently, the perturbation region of the elastoplastic medium becomes wider than the perturbation region of a nonlinearly compressible ideal medium.

It can be seen from Fig.5 that in the case of soil modeling in a nonlinearly compressible medium, as compared to the elastoplastic problem, the load profile  $\sigma_0(t)$ , found from the solution in the reverse way, changes relatively slowly in time.

In addition, all medium parameters at  $r = r_0$ , depending on time  $t$ , have a decaying character. A similar law of variation of the parameters  $\sigma_{rr} = -p, \sigma_{\varphi\varphi}, U_t = U^1$  in time is observed at  $r > r_0$ . However, at  $r > r_0$ , the intensity of the above parameters is somewhat weaker than at  $r = r_0$ . The curves in Figs. 6-7 show that  $\sigma_{rr}, U_t$ , depending on the spatial coordinate  $r$  at fixed moments of time  $t = 0.15 * 10^{-3}, 0.30 * 10^{-3}, 0.45 * 10^{-3}$  sec. excluding  $\sigma_{rr}$  of the elastoplastic medium (Fig. 7, the solid line) change, mainly according to the linear law.

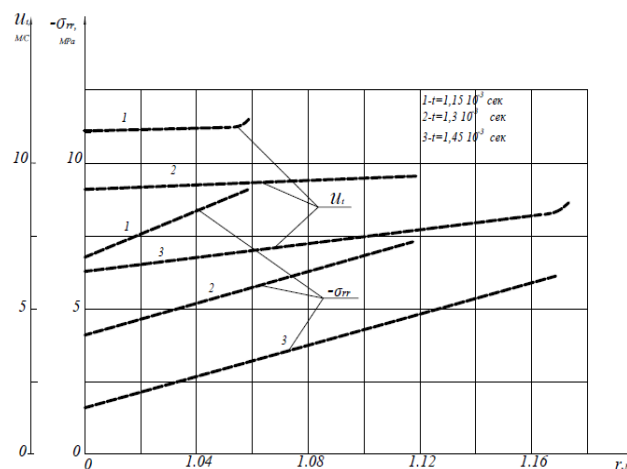


**Figure 6.** The change in pressure  $P = \sigma_{rr}$  and mass velocity city  $U_t$ , depending on coordinate  $r$  at fixed times  $t = 0,15 \cdot 10^{-3}$  sec (curve 1),  $0,30 \cdot 10^{-3}$  sec (curve 2),  $0,45 \cdot 10^{-3}$  sec (curve 3).

The stress  $\sigma_{rr}$  calculated for an elastoplastic medium is the smallest in absolute value. The same picture occurs when the stresses  $\sigma_{rr}^*$ ,  $\sigma_{\varphi\varphi}^*$  and the mass velocity  $U_t^*$  along the wave front depending on time change (Fig. 8). In order to compare the results of similar and numerical methods on a computer, using the method of characteristics, we calculated the problem of wave propagation in soil for the load  $\sigma_0(t)$  previously obtained analytically by the inverse method (solid line in Fig. 5). Comparing the results of calculations on the distribution of the medium's parameters along the shock wave front, we note that the results of the method of characteristics (dashed lines with circles in Fig. 8) satisfactorily coincide with the analytical solution of the problem.

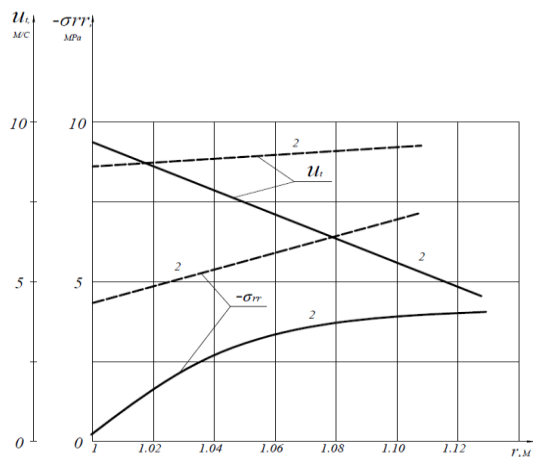


**Figure 7.** Change in radial stress  $-\sigma_{rr}$  and mass velocity depending on the coordinate  $t = 0.30.10$  sec for elastoplastic (solid) and ideal nonlinearly compressible plastic (dashed lines) medium

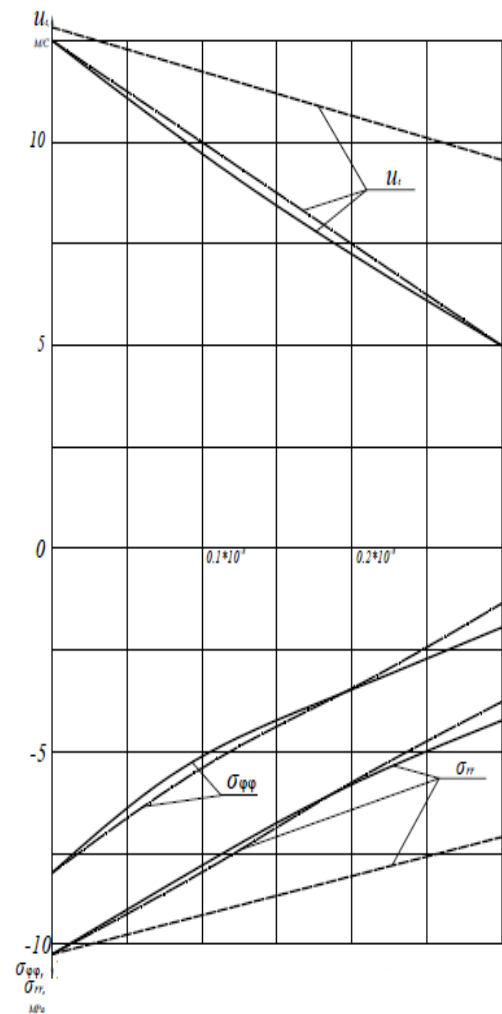


**Figure 8.** Change in stresses  $\sigma_{rr}^*$ ,  $\sigma_{\varphi\varphi}^*$  and mass velocity  $U_t$  at the wave front as a function of time elastoplastic (solid) and ideal non-compressible plastic (dashed lines) medium, ;dashed lines with circles are the results of the method of characteristics

Thus, it should be noted that if the velocity of the shock front is a monotonically decreasing function of time, then all the parameters of the medium in the disturbance region, including the load profile at the cavity boundary, are also obtained by the damped function of time. The stress components and the mass velocity of the medium at the boundary of the cavity decrease faster over

time than at the wave front. In the study it was found that with an increase in coefficients  $\alpha_1$ ,  $\alpha_2$ ,  $\beta_1, \beta_2$ , the stress components increase, and with an increase in Young's modulus,  $E_1, E_2$  they damp. However, the effect of  $E_2$  on the distribution of medium parameters is weaker than of  $E_1$ .

#### 4. Conclusions

Based on the results of the studies, the following conclusions can be drawn:

1. The problem of a spherical shock wave propagation in an elastoplastic medium is solved analytically and numerically by the method of characteristics on the basis of the deformation theory, taking into account the generalized equations of state of the medium. The study showed that for an elastic-plastic medium, a change in the values of Young's moduli  $E_1$  and  $E_2$  noticeably affects the profile  $\sigma_0(t)$ .
2. The propagation of a spherical shock wave in an elastoplastic medium with a more complex equation of state for medium forming  $\sigma_i = \sigma_i(\varepsilon, \varepsilon_i)$  was investigated by the inverse method. The calculation results showed that in this case the monotonically decreasing load profile  $\sigma_0(t)$  turns out to be steeper and faster decreasing in time than in the case  $\sigma_i = \sigma_i(\varepsilon_i)$  and substantially depends on the shape of the spherical load–unload shock wave.
3. An analysis of the results of computer calculations shows that an account for nonlinear elastic shock diagrams  $\sigma(\varepsilon)$  at  $\theta = \pi/2$  leads to an increase in the circular stress wave  $\sigma_{\theta\theta}$  compared with an elastic medium with Young's modulus  $E$  calculated in tangent to the curve  $\sigma(\varepsilon)$  for  $\varepsilon \rightarrow 0$ . If  $E$  is determined “by chord” of the curve  $\sigma(\varepsilon)$ , then the value of  $\sigma_{\theta\theta}$  for  $\theta = \pi/2$  is the greatest.
4. It was found that the stress concentration on the spherical cavity is higher than on the cylindrical one. Due to irreversible properties and complex equations of state of the medium, the stress distribution on the spherical cavity changes significantly, in contrast to the case of diffraction of an elastic wave on the cavity, and transient wave processes turn out to be long and complex in structure.

#### References

- [1] Rakhmatulin H A, Sagomonyan A Ya and Alekseev N A 1964 Issues of soil dynamics. M.: Publishing House of Moscow State University p 239.
- [2] Rakhmatullin H A 1958 On the propagation of an explosion shock wave in soils - M.: Publishing House of the Academy of Sciences of the USSR.
- [3] Investigation of the mechanical properties of soils under conditions of triaxial compression at an elevated level of stress. Report of the Moscow Institute of Mathematics and Mathematics named after V.V. Kuybyshev, No. 320 M., 1972 - p.68.
- [4] Novatsky V K 1978 Wave problems of the theory of plasticity. M. : Publishing houses Mir p.307.
- [5] Luntz Y A 1949 Propagation of spherical elastoplastic waves. // PMM, T.13 No. 1p.129.
- [6] Atabaev K, Abduzhalilov Sh G and Turaev N 1988 On the propagation of one-dimensional waves in a medium with nonlinear unloading // DAN Uz.SSR, No. 9 pp.20 - 23.
- [7] Dashevsky M A 1976 Calculation of cavities in an elastic medium on the action of an unsteady plane compression wave. // Structural mechanics and calculation of structures, No. 3 pp. 44 - 46.
- [8] Korotkov P F 1976 Numerical study of an explosion in an elastoplastic medium and some modeling issues / DAN SSSR. T.228. No. 1.
- [9] Broad G L 1975 Calculations of explosions on a computer. Underground explosions. - M.: MIR Publishing House.
- [10] Kato S, Hashimoto S and Uemichi A 2010 Propagation characteristics of shock waves driven by gaseous detonation waves *Shock Waves vol.20* pp 479–489. <https://doi.org/10.1007/s00193-010-0279-6>
- [11] Xiao W, Wei H and Feng L 2017 Investigation on the cavitation effect of underwater shock near different boundaries *China Ocean Eng. Vol.31.* pp.396–407 <https://doi.org/10.1007/s13344-017-0046-x>

- [12] Winter K O and Hargather M J 2019 Three-dimensional shock wave reconstruction using multiple high-speed digital cameras and background-oriented schlieren imaging. *Exp Fluids* 60, 93. <https://doi.org/10.1007/s00348-019-2738-x>
- [13] Liang S M, Wang J S and Chen H 2002 Numerical study of spherical blast-wave propagation and reflection. *Shock Waves* vol.12 pp 59–68 <https://doi.org/10.1007/s00193-002-0142-5>
- [14] Jiang J, Blair D P and Baird G R 1995 Dynamic response of an elastic and viscoelastic full-space to a spherical source *Int. J. for Num. and An.Meth. in Geom.* pp 181-193. **DOI:** 10.1002/nag.1610190303
- [15] Chattopadhyay A and Michel V A 2006 Model for spherical SH wave propagation in self-reinforced linearly elastic media [Archive of Applied Mechanics.](#) pp 113–124 doi.org/10.1007/s00419-005-0417-2
- [16] Kandula M and Freeman R 2008 On the interaction and coalescence of spherical blast waves. *Shock Waves* vol.18 pp 21–33 <https://doi.org/10.1007/s00193-008-0134-1>
- [17] Grigoryan S.S. About the action of a strong underground explosion in dense rock / S.S. Grigoryan, Y.A. Pachevsky // DAN USSR. - 1973. - T. 212. - No. 2.
- [18] Chen J-Y, Peng C and Lien F-S 2019 Simulations for three-dimensional landmine detonation using the SPH method *Int. J. of Imp. Eng.* Vol.126 pp 40-49 **DOI:** 10.1016/j.ijimpeng.2018.12.004
- [19] Lomise G.M. The study of the laws of development of the stress-strain state of a sandy base during flat deformation / Foundations, foundations and soil mechanics. - 1972. - No. 1.
- [20] Wu C,Hao H, Lu Y and Sun S 2004 Numerical simulation of structural responses on a sand layer to blast induced ground excitations *Computers and Structures* Vol.82, Issue 9-10 pp 799-814 **DOI:** 10.1016/j.compstruc.2004.01.003
- [21] Pontalier Q, Loiseau J, Goroshin S and Frost D L 2018 Experimental investigation of blast mitigation and particle–blast interaction during the explosive dispersal of particles and liquids *Shock Waves* Vol. 28 Issue 3 pp 489-511. **DOI:** 10.1007/s00193-018-0821-5
- [22] Chen H, Jin F and Fan H 2013 Elastic responses of underground circular arches considering dynamic soil-structure interaction: A theoretical analysis. [Acta Mechanica Sinica Sin](#) vol.29 pp 110–122 <https://doi.org/10.1007/s10409-013-0012-7>